

Supplementary Materials for

Mechanically transformative electronics, sensors, and implantable devices

Sang-Hyuk Byun, Joo Yong Sim, Zhanan Zhou, Juhyun Lee, Raza Qazi, Marie C. Walicki, Kyle E. Parker, Matthew P. Haney, Su Hwan Choi, Ahnsei Shon, Graydon B. Gereau, John Bilbily, Shuo Li, Yuhao Liu, Woon-Hong Yeo, Jordan G. McCall, Jianliang Xiao, Jae-Woong Jeong*

*Corresponding author. Email: jjeong1@kaist.ac.kr

Published 1 November 2019, *Sci. Adv.* **5**, eaay0418 (2019)

DOI: 10.1126/sciadv.aay0418

The PDF file includes:

- Note S1. Theoretical analysis of phase transition time for thawing
 - Note S2. Fabrication of transformative electronics with flexible, stretchable electrode arrays
 - Note S3. Fabrication of transformative electronics integrated with a stretchable PCB
 - Note S4. Fabrication of neural probe with variable stiffness
 - Fig. S1. Design and application of a transformative electronics that can convert between an EMG sensor and a handheld touch sensor.
 - Fig. S2. Design of testbed transformative platforms for mechanical studies.
 - Fig. S3. Characterization of the degree of supercooling.
 - Fig. S4. Thermal characterization of gallium-based transformative platform using IR camera during thawing process and freezing process.
 - Fig. S5. Design of transformative electronics that can convert between a rigid tabletop clock and a stretchable wearable sensor with characterization.
 - Fig. S6. Mechanical simulation of bending stiffness of the transformative electronics that appeared in Fig. 3E.
 - Fig. S7. Fabrication process of a transformative pressure sensor.
 - Fig. S8. Transformative resistive pressure sensor built with a gallium frame.
 - Fig. S9. Response time of the pressure sensor in rigid and soft mode.
 - Fig. S10. Design and implementation of TES optical neural probe for behavioral experiments with wireless control.
- Legends for movies S1 to S4

Other Supplementary Material for this manuscript includes the following:

(available at advances.sciencemag.org/cgi/content/full/5/11/eaay0418/DC1)

Movie S1 (.mp4 format). Movie of a transformative electronics transforming between a rigid tabletop clock and a wearable sensor.

Movie S2 (.mp4 format). Movie of a transformative pressure sensor with variable deformability.
Movie S3 (.mp4 format). Movie of a transformative pressure sensor: Application demonstration in rigid and soft modes.
Movie S4 (.mp4 format). Movie of a transformative neural probe penetrating a mouse brain in rigid mode.

Supplementary Note

Note S1. Theoretical analysis of phase transition time for thawing

The phase transition time for thawing transformative electronics system (TES) testbed platforms in Fig. 2 was calculated from Fourier's law of conduction. The testbed platforms were comprised of a 1.5 mm thick gallium frame and 0.5 mm thick silicone encapsulant. Assuming that thermal conduction from the hot-plate is a dominant factor of heat transfer, the heat transfer rate through conduction can be simplified as follows

$$q = -k_{encap}A \frac{T - T_{th}}{t_{encap}} = C_{Ga} \frac{dT}{dt} \quad (S1)$$

where T is the temperature of gallium frame, k_{encap} is the thermal conductivity of the silicone encapsulant, A is the area of gallium frame, T_{th} is the thawing temperature, t_{encap} is the gallium frame thickness, and C_{Ga} is the heat capacity of the gallium frame. Let T_m be the melting point of gallium (302.95 K). Then, the transient temperature of the gallium frame can be expressed as

$$\int_{T_0}^T \frac{1}{T - T_{th}} dT = \int_0^t -\frac{1}{C_{Ga}} \frac{k_{encap}A}{t_{encap}} dt \quad (\text{define } \alpha \equiv \frac{k_{encap}A}{C_{Ga}t_{encap}}) \quad (S2)$$

where T_0 is the initial temperature of the TES, which is initially below T_m . The temperature of the gallium frame is

$$T = T_{th} - (T_{th} - T_0)e^{-\alpha t} \quad (S3)$$

The time to reach the phase transition temperature, t_{c1} , can be expressed as

$$t_{c1} = \frac{1}{\alpha} \ln \frac{T_0 - T_{th}}{T_m - T_{th}} \quad (S4)$$

Here, t_{c1} is equal to the time at which the phase transition begins. To calculate the time required for phase transition, the energy to be provided, that is the enthalpy of fusion, can be calculated by

$$\int_{t_{c1}}^{t_{thaw}} -k_{encap}A \frac{T_m - T_{th}}{t_{encap}} dt = Q_p \quad (S5)$$

where Q_p is the heat of fusion for the gallium frame and t_{thaw} is the time at which the phase transition ends. Then, t_{thaw} can be calculated by

$$t_{thaw} = t_{c1} + Q_p \frac{t_{encap}}{(T_{th} - T_m)k_{encap}A} \quad (S6)$$

Here, the heat of fusion, Q_p , is $\rho \cdot t_{Ga} \cdot A \cdot L$ where ρ is the density of gallium, t_{Ga} is the thickness of the gallium frame, and L is the latent heat. Because the heat of fusion ($5590 \text{ J} \cdot \text{mol}^{-1} \cdot \text{K}^{-1}$) is two orders of magnitude larger than the heat capacity of gallium ($25.86 \text{ J} \cdot \text{mol}^{-1} \cdot \text{K}^{-1}$), the time to reach the transient temperature (t_{c1}) is negligible compared to the phase transition time. The expression for the phase transition time can be written as

$$t_{transition} = t_{thaw} \sim t_{encap} \cdot \rho \cdot t_{Ga} \cdot L / (k_{encap}(T_{th} - T_m)) \quad (S7)$$

Therefore, the phase transition time has an approximate relation as

$$t_{transition} \propto t_{encap} \cdot t_{Ga} / (T_{th} - T_m) \quad (S8)$$

Note S2. Fabrication of transformative electronics with flexible, stretchable electrode arrays

To fabricate stretchable electrode arrays, which can be used for both EMG and touch sensors (Fig. 1), 10 μm thick PDMS layer was first formed on a glass slide (75 mm \times 50 mm \times 1 mm) by spin-coating and curing PMDS at 70 $^{\circ}\text{C}$ for 60 min. A thin layer of polyimide (1.2 μm in thickness, PI 2545, HD MicroSystems) was then spin-casted on the PDMS-coated glass substrate and cured at 250 $^{\circ}\text{C}$ for 60 min. E-beam evaporation of Cr/Au (5nm/200nm in thickness) followed by photolithographic patterning created electrodes and stretchable interconnects. Encapsulation of these patterns with another PI layer (1.2 μm in thickness) positioned the electrode layer at the neural mechanical plane to protect the metal structures from the bending stress. Both the top and the bottom PI layers were then etched using photolithography and reactive ion etching (KVIA-3008DC, KOREAVAC) to define stretchable electrodes encapsulated with PI. For transfer printing, the device was picked up using water-soluble tape (ASWT-2, Aquasol) and deposited with Cr/SiO₂ (5 nm/60 nm) onto the bottom before being printed on the surface of the transformative platform illustrated in the previous fabrication step. This SiO₂ layer served as an adhesion promotor when the device was printed on the silicone layer of the transformative platform. Finally, the fabrication of the transformative electronics shown in Fig. 1 was completed by removing the water-soluble tape with water.

Note S3. Fabrication of transformative electronics integrated with a stretchable PCB

For transformative electronics shown in Fig. 3, a stretchable printed circuit board (PCB) and a heater was fabricated on a Kapton film (120 μm in thickness) with copper interconnects (18 μm in thickness). A BLE (Bluetooth low energy) microcontroller (Simpler, RF Digital), OLED screen (SSD1306, Adafruit), UV sensor (SI1145-A10-GMR, Silicon Labs), thermistor (10 k Ω), a voltage regulator (NCP4624DMU30TCG, ON Semiconductor), and active and passive components of SMD type (i.e. transistor, LED, resistor, and capacitor) were mounted on the PCB using a low temperature soldering paste (SMDLTMFP10T5, ChipQuik). Then, the PCB, the heater, and the transformative platform were integrated together and encapsulated with silicone (Ecoflex 00-30, Smooth-On) to complete the transformative electronics in Fig. 3 (For photographic illustration, see fig. S5).

Note S4. Fabrication of neural probe with variable stiffness

The fabrication of a μ -ILED neural probe started with defining metal electrodes on PET (6 μm thick) by deposition of Cr/Au (5 nm/300 nm), followed by photolithography and metal etching. A μ -ILED was attached onto the metal electrodes with silver conductive epoxy (8331 series, MG Chemicals). For the gallium-based transformative platform, liquid gallium was casted and solidified in a 50 μm thick Kapton film mold sandwiched between the two glass slides. Then the probe-shaped gallium was encapsulated with silicone elastomer (30 μm thick, Ecoflex 00-30, Smooth-On). Finally, the μ -ILED probe was laminated on the transformative platform and coated with parylene C (6 μm) for water-proofing and biocompatibility.

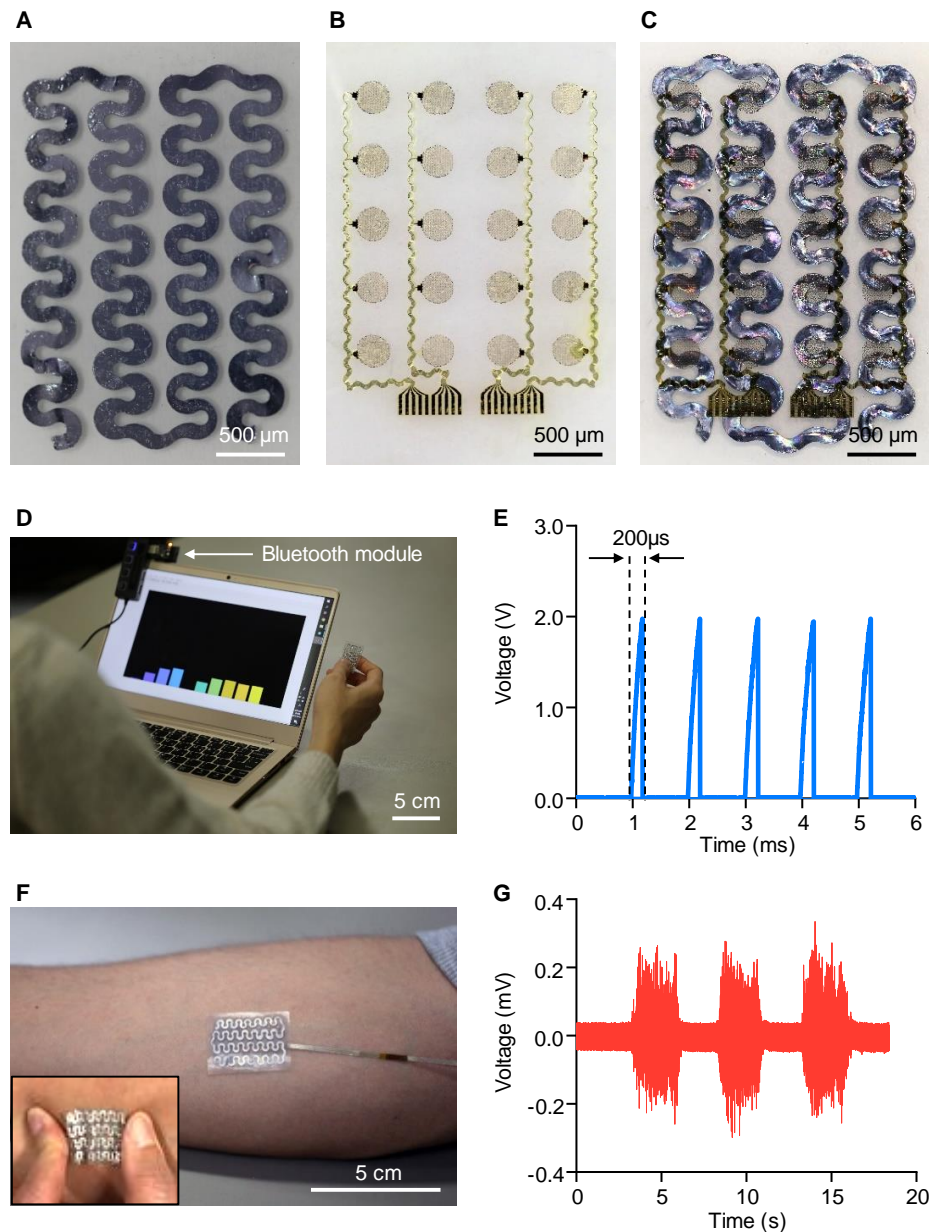


Fig. S1. Design and application of a transformative electronics that can convert between an EMG sensor and a handheld touch sensor. (A, B) Images illustrating key components of the device composed of a gallium frame encapsulated with silicone (Ecoflex) as a transformative platform (A) and stretchable gold electrodes as an EMG sensor (B). (C) Image of a completed transformative electronics, fabricated by transfer-printing the stretchable EMG sensor on the transformative platform. (D) Demonstration of the device in rigid mode as a handheld touch sensor for remote control of the volume of a computer. The device is connected to a Bluetooth module so that it can communicate with a laptop computer to control the user-interface of a music player. (E) Voltage signals measured at an input port of the Bluetooth module when touching the sensor in (D). Measurements were taken every 1 ms. (F) Demonstration of the device in soft mode as a wearable sensor measuring EMG signals from a forearm. (G) Measured EMG signals in (F). Photo credit: Jae-Woong Jeong (A to C) and Sang-Hyuk Byun (D and F).

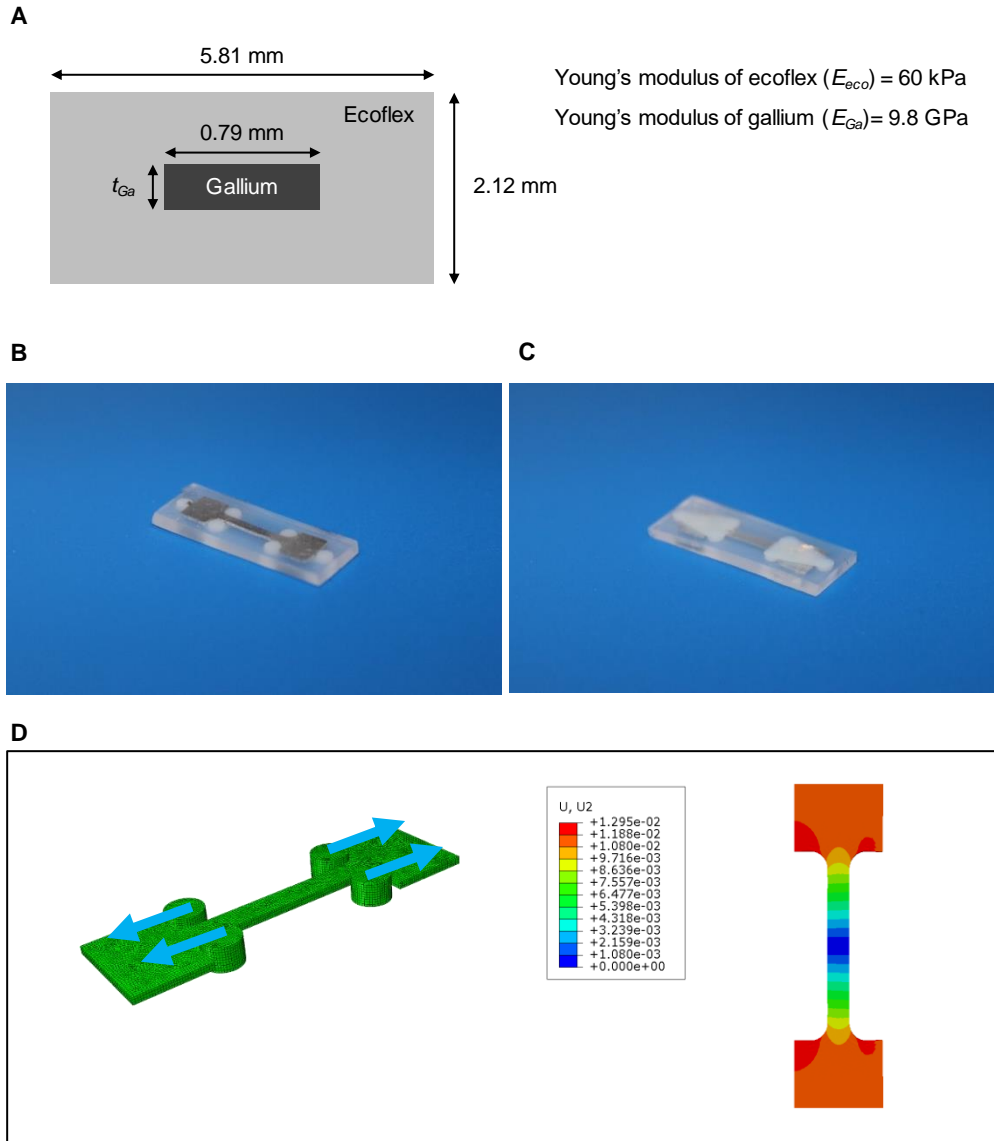


Fig. S2. Design of testbed transformative platforms for mechanical studies. (A) Schematic diagram showing a cross sectional view of mechanical test sample. (B, C) Images of a sample viewed from the top (B) and bottom (C). 3D printed triangular plastic pieces are used to securely hold a dogbone-shaped sample at both ends to apply stress only to the sample body during mechanical testing. This approach helps accurate measurement of elastic modulus from the sample body structure. (D) Finite element analysis (FEA) simulation that shows distributed stress along the body of a dogbone-shaped sample, verifying the mechanical isolation of the sample body part from the holder part during the measurements. Photo credit: Zhanan Zhou.

Thickness of gallium = 1500 μm , thickness of ecoflex = 500 μm

T_{th} = The highest temperature gallium experienced in thawing

Freezing temperature

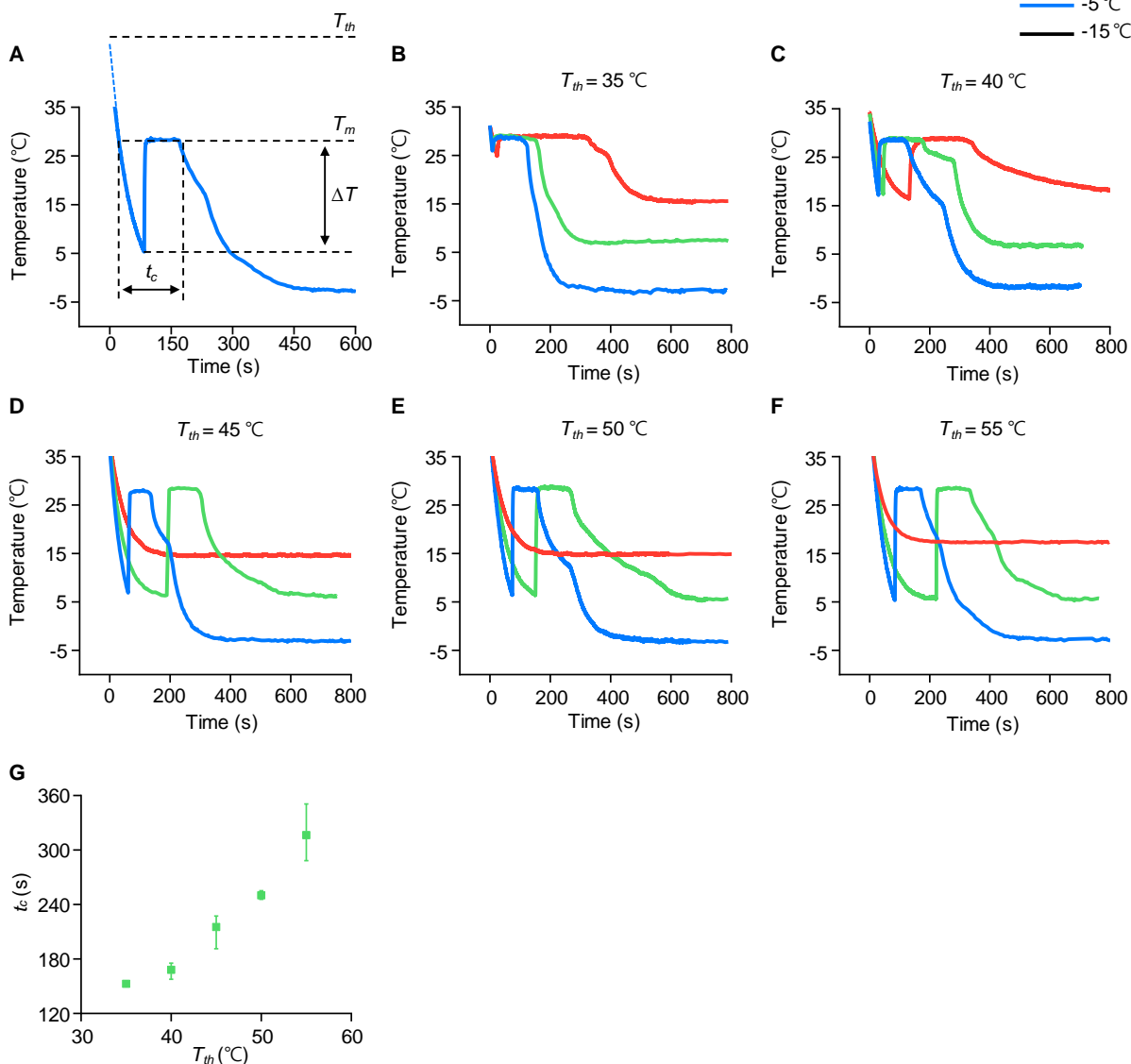
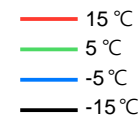


Fig. S3. Characterization of the degree of supercooling. (A) Temperature change characteristics during the freezing process with definition of terminologies. t_c , T_{th} , T_m , and ΔT represent the characteristic phase transition time, the thawing temperature, the melting point of gallium, and the difference between T_m and the nucleation temperature (the lowest temperature during supercooling). (B–F) Plots illustrating the degree of supercooling (ΔT) depending on thawing temperature (T_{th}). (G) Characteristic transition time (t_c) as a function of applied thawing temperature (T_{th}) before freezing samples at 5 °C.

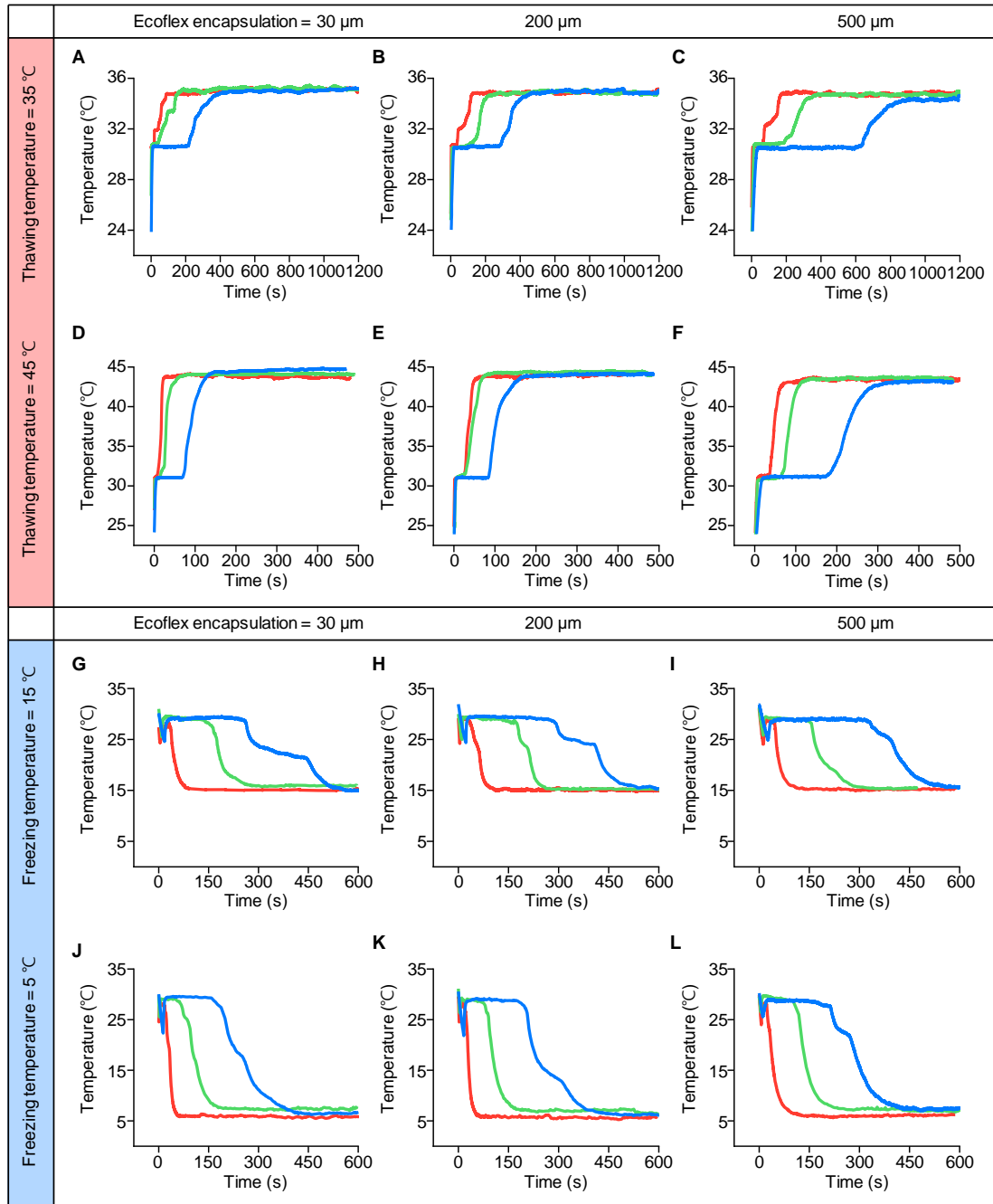


Fig. S4. Thermal characterization of gallium-based transformative platform using IR camera during thawing process and freezing process. (A–F) Plots illustrating phase transition of platforms, depending on the thawing temperature and the thicknesses of encapsulation silicone (Ecoflex) and gallium. (G–L) Plots illustrating phase transition of platforms, depending on the freezing temperature and the thicknesses of encapsulation silicone (Ecoflex) and gallium. Note that the initial ‘soft’ platform with liquid gallium was prepared by applying thawing temperature of 35 °C for 20 min.

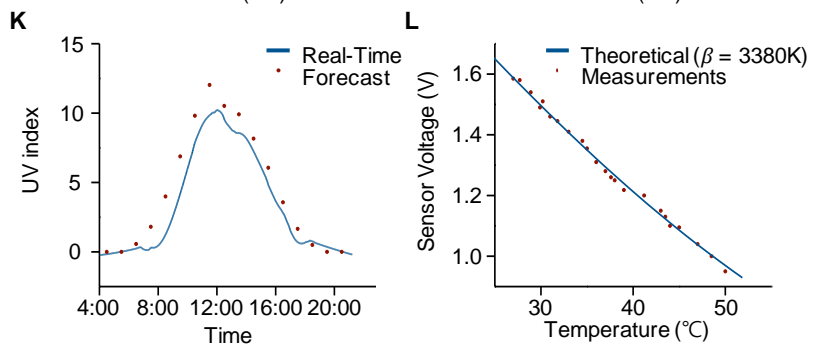
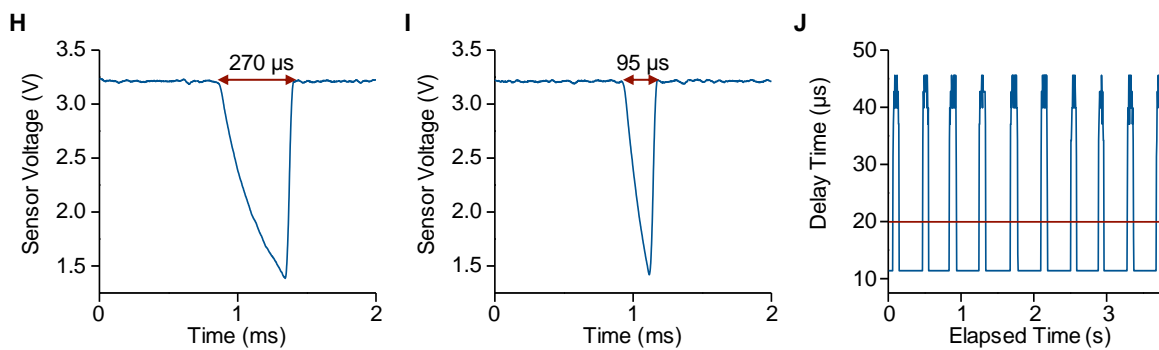
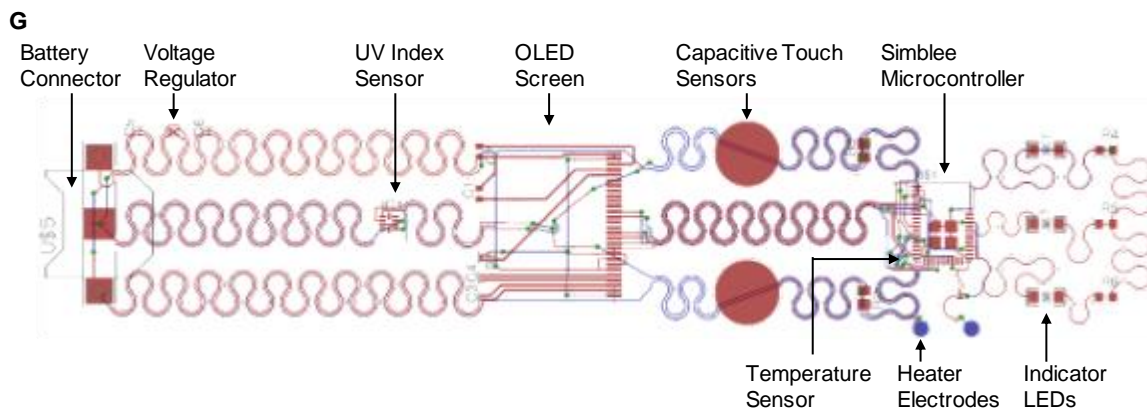
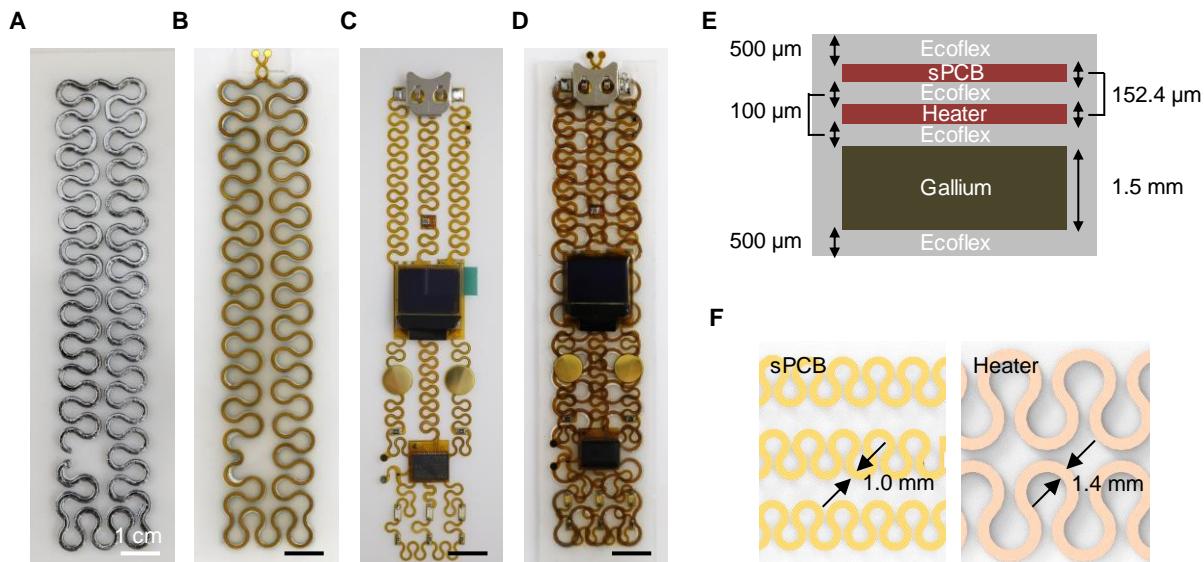


Fig. S5. Design of transformative electronics that can convert between a rigid tabletop clock and a stretchable wearable sensor with characterization. (A–D) Images illustrating the fabrication process flow for integrating different structural layers of the device. (A) Prepare a gallium frame and encapsulate it with Ecoflex to make a transformative platform. (B) Mount a stretchable heater layer on the top of the transformative platform. (C) Prepare stretchable printed circuit board (PCB) assembled with electronic components. (D) Integrate the PCB onto the transformative platform in (B) and encapsulate with Ecoflex. (E) Schematic diagram showing a cross-sectional view of the device with dimensional information. (F) Schematic diagram showing a top view of the device with dimensional information. (G) PCB layout with featured components. Red, blue, and dark grey color represent the top layer, the bottom layer, and the board outline, respectively. (H–L) Characterization of sensors in the transformative electronics. (H, I) Response of the capacitive touch sensor (H) with and (I) without finger touch. Before the measurement, the net is pulled high with a 1 M Ω resistor. Measurement begins when the net is pulled low in software. The amount of time taken for the net to reach logical low is recorded, and the measured pin is tri-stated in software to return the net to its original state. (J) Response of the capacitive touch sensor to ten quick touches. The vertical axis is the time taken for the voltage at the microcontroller input pin of decay to logical low. If the measured decay time is longer than a certain cutoff, it is accepted as a valid touch. The cutoff was selected to eliminate false readings from moving a finger close to the sensor without touching it. (K) Characterization of UV index sensor with forecasted information for Boulder, Colorado, provided by National Center for Atmospheric Research. (L) Characterization of temperature sensor. The temperature sensor consisted of a 10 k Ω NTC-type thermistor in series with a 10 k Ω resistor. 3.3 V of voltage was applied across the circuit, and voltage was measured at the junction of the two resistors. Theoretical response of the circuit was computed by using the beta coefficient of the thermistor to compute the resistance of the thermistor for the temperature range of 25 °C to 50 °C. Photo credit: Sang-Hyuk Byun.

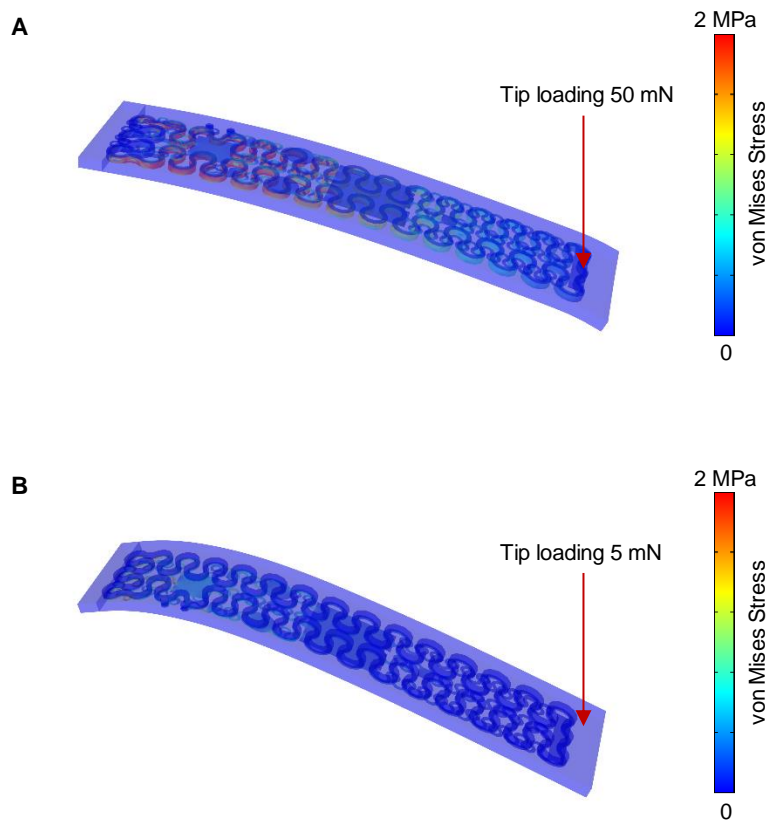


Fig. S6. Mechanical simulation of bending stiffness of the transformative electronics that appeared in Fig. 3E. Stress distribution of the device under tip loading in rigid (A) and soft mode (B).

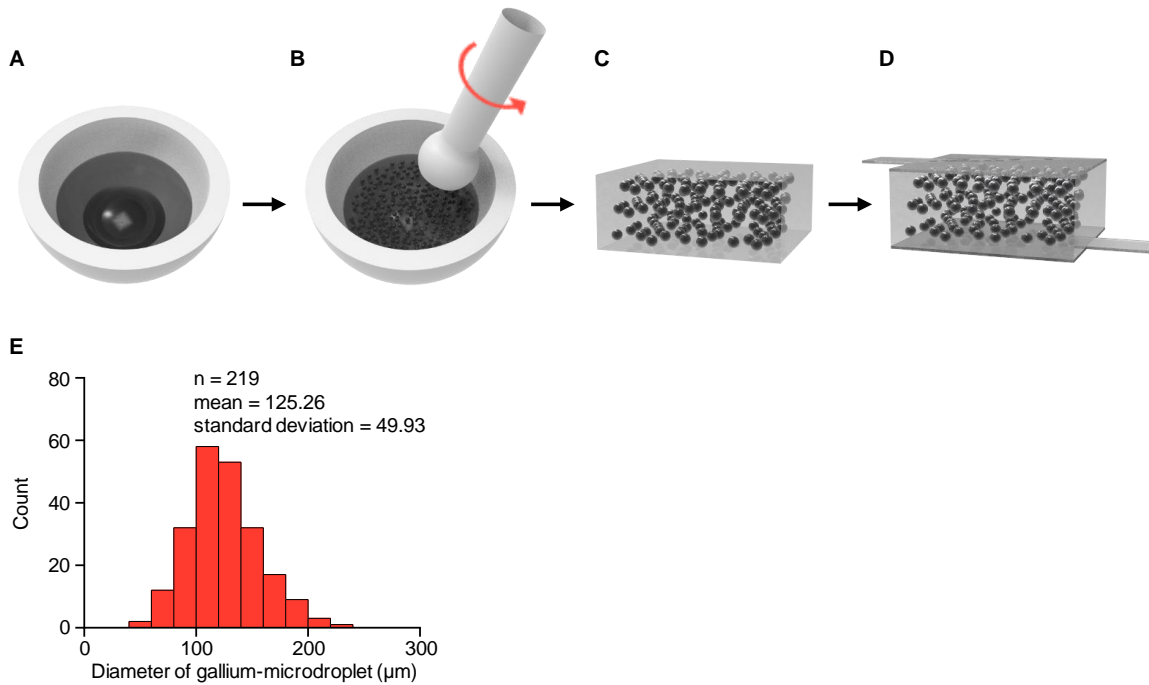


Fig. S7. Fabrication process of a transformative pressure sensor. (A) Prepare liquefied gallium and uncured PDMS (15:1 elastomer:curing agent weight ratio) at a volume ratio of 1:1. (B) Mix gallium and PDMS for ~10 min with a mortar and pestle. (C) After curing at 70 °C for 60 min, cut the composite for the targeted dimensions. (D) Attach ITO-covered PET or copper foil on top and bottom of the composite. (E) Diameter distribution of gallium-microdroplets in gallium-elastomer composite presented in Fig. 4C.

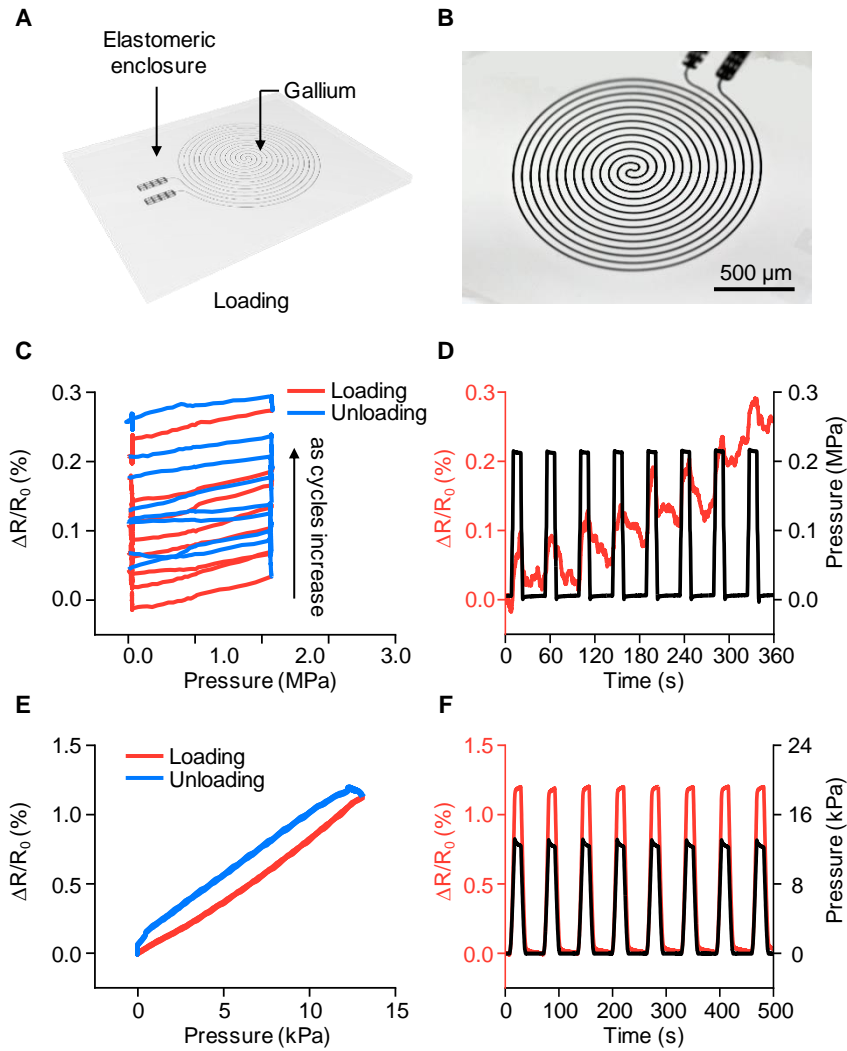


Fig. S8. Transformative resistive pressure sensor built with a gallium frame. (A) Schematic diagram showing the design of a gallium frame-based pressure sensor fabricated by injection of gallium into a microfluidic channel. (B) Optical image of a pressure sensor integrating a 50 μm thick gallium frame. (C) Relative resistance changes of the pressure sensor in rigid mode with repetitive applied pressure, showing inconsistent sensing response. (D) Relative resistance changes of the pressure sensor in rigid mode with applied pressure as a function of time. The sensor output gradually increases for the same applied pressure as cycles increase due to the ductility of gallium. (E) Relative resistance changes of the pressure sensor in soft mode with repetitive applied pressure, showing linear sensing response with low hysteresis. (F) Relative resistance changes of the pressure sensor in soft mode with applied pressure as a function of time.

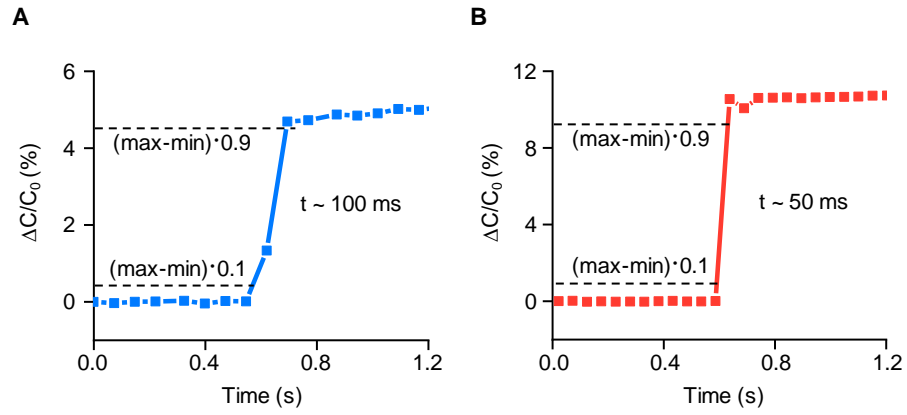


Fig. S9. Response time of the pressure sensor in rigid (**A**) and soft (**B**) mode.

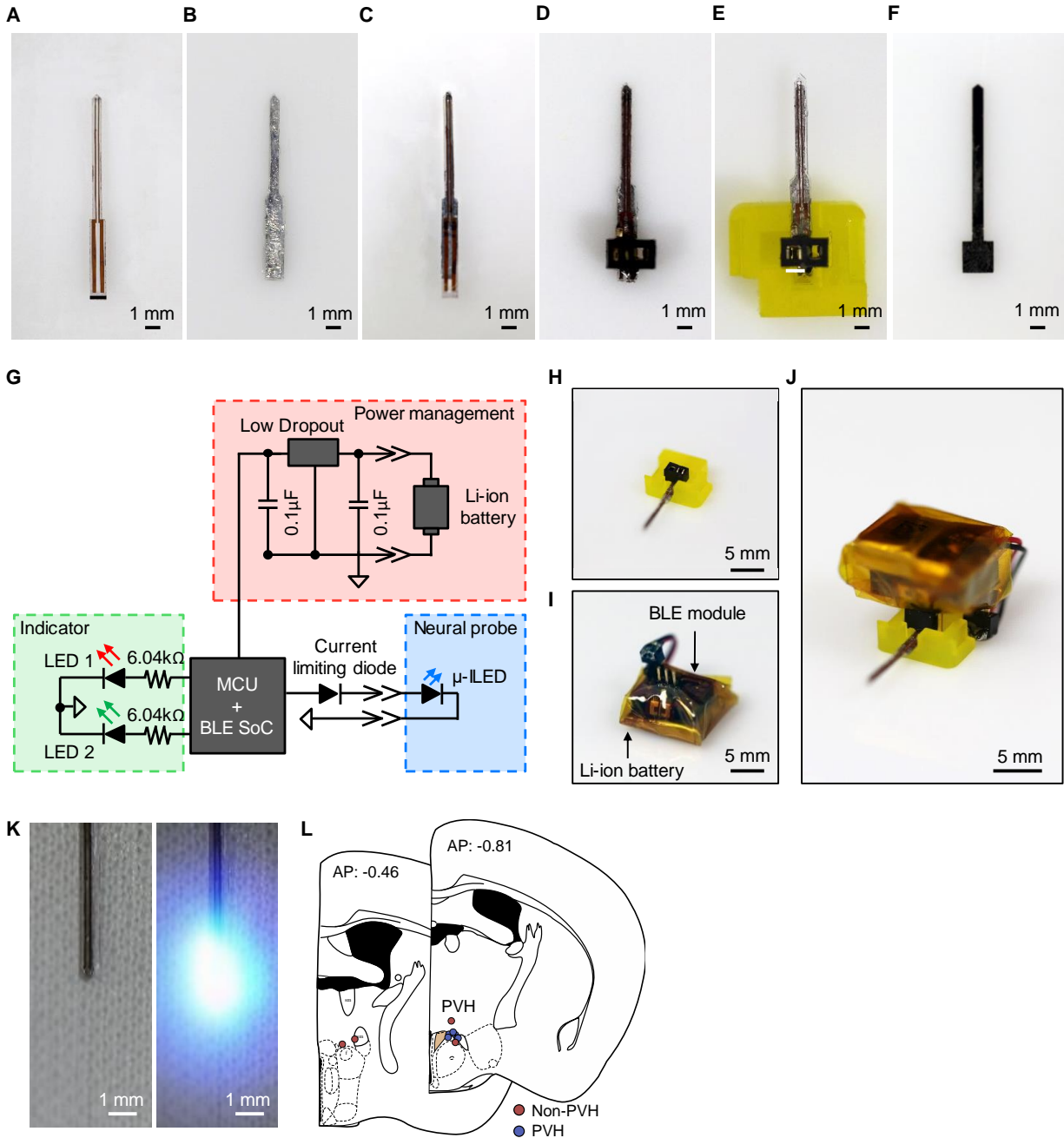


Fig. S10. Design and implementation of TES optical neural probe for behavioral experiments with wireless control. (A – E) Fabrication procedure. (A) Fabricate a μ -ILED probe on a PET substrate. (B) Prepare a gallium-based transformative platform encapsulated with silicone elastomer. (C) Integrate a μ -ILED probe on the gallium transformative platform. (D) Attach a pin connector on top of the electrodes of the neural probe for power supply or for connection of a wireless module. (E) Mount the probe on a 3D-printed supporter to facilitate the handling. (F) Rigid control probe made of Tungsten to compare immunoreactive response with the one caused by the TES probe shown in (E). (G) Circuit diagram of a Bluetooth Low Energy (BLE) wireless module. (H, I) Photographs of a TES optical neural probe (H) and a wireless module (I). (J) Optical image of a wireless neural probe after assembly. (K) Functional

demonstration of TES-based neural probe prior to implantation. **(L)** Hit map of TES neural probe placements for the experiments in Fig. 5, H to L. Blue dots represent LED location on the devices in PVH animals and red dots represent LED location on the devices in non-PVH animals. Photo credit: Sang-Hyuk Byun.

Movie S1. Movie of a transformative electronics transforming between a rigid tabletop clock and a wearable sensor.

Movie S2. Movie of a transformative pressure sensor with variable deformability.

Movie S3. Movie of a transformative pressure sensor: Application demonstration in rigid and soft modes.

Movie S4. Movie of a transformative neural probe penetrating a mouse brain in rigid mode.